

# Zero-Point Vacancy Concentration in a Model Quantum Solid: A Reversible-Work Approach

Renato Pessoa · Maurice de Koning ·  
Silvio Antonio Vitiello

Received: 11 November 2008 / Accepted: 23 February 2009 / Published online: 6 March 2009  
© Springer Science+Business Media, LLC 2009

**Abstract** We investigate the influence of anharmonic effects on the zero-point vacancy concentration in a boson system model in the solid phase at  $T = 0$  K. We apply the reversible-work method to compute the vacancy formation free energy and the vacancy concentration in the system. A comparison of our results with those obtained using the harmonic approximation show that anharmonic effects reduce the formation free energy by  $\sim 25\%$ , leading to an increase of the zero-point vacancy concentration by more than an order of magnitude.

**Keywords** Quantum solids · Vacancy concentration · Anharmonic effects · Reversible work method

## 1 Introduction

In this paper we continue the study of quantum solids formed by bosons. Our aim is to perform a vacancy-concentration calculation and quantify the importance of anharmonic effects in its value by introducing the reversible work (RW) method [22] in the context of such systems. The importance of these effects in the solid phase of a system of light bosons is twofold. They would manifest themselves both due to significant zero-point motion and the local breaking of lattice symmetries in the presence of a vacancy [13, 14, 22]. In this work we consider a simple model system for which the exact ground-state wave function is of the Jastrow form

$$\psi_J(R) = \exp \left[ -\frac{1}{2} \sum_{i < j}^N u(r_{ij}) \right] / Q_N^{1/2}, \quad (1)$$

---

R. Pessoa (✉) · M. de Koning · S.A. Vitiello  
Instituto de Física Gleb Wataghin, Caixa Postal 6165,  
Universidade Estadual de Campinas, UNICAMP 13083-970, Campinas, SP, Brazil  
e-mail: [rpessoa@ifi.unicamp.br](mailto:rpessoa@ifi.unicamp.br)

M. de Koning  
e-mail: [dekoning@ifi.unicamp.br](mailto:dekoning@ifi.unicamp.br)

S.A. Vitiello  
e-mail: [vitiello@ifi.unicamp.br](mailto:vitiello@ifi.unicamp.br)

where  $R \equiv \{\mathbf{r}_1, \mathbf{r}_2, \dots, \mathbf{r}_N\}$  stands for the  $N$  coordinates of the particles and  $Q_N$  is a normalization constant. We wish to demonstrate that the RW method provides a sound approach to pursue our aims, allowing a reliable calculation of defect concentrations in quantum solids formed by bosons. Moreover we demonstrate that our method is efficient, enabling a systematic elimination of finite-size effects associated with spurious vacancy-vacancy interactions in the results.

It is not our intention to make claims about real systems using such simple model described by the wave function in (1). However we note that a wave function of this form has been employed [16, 26] in the past to describe a system of helium atoms in the solid phase using the so called pseudopotential  $u(r) = (b/r)^n$  of the McMillan form. In order to consider helium atoms in bulk, more reliable translational invariant descriptions of this system in the solid phase exist [24, 34]. Here we adhere to the model system of (1) in order to keep our calculations as simple as possible.

Nevertheless our results might be of interest in the context of the systems formed by helium atoms in view of the possible role that lattice vacancies could play in relation to the recent experimental observations of nonclassical rotational inertia (NCRI) [17, 18]. Moreover it has been noticed that the NCRI has an unusual dependence on density [19] and that it might be related to an unexpected mechanical behavior under elastic deformations [12]. One of the possible interpretation of these phenomena is the existence of a supersolid phase, which presents long-range order, spontaneous translational and rotational symmetry breaking characteristic of a crystal but displaying superfluid-like behavior present in the low-temperature liquid phase. The pioneering theoretical proposals of a supersolid phase [3, 10] predict that vacancies are required for quantum crystals to exhibit superfluid behavior. More recently, Anderson, Brinkman and Huse [2] have supported this view based on experimentally observed behavior of the specific heat [8]. From the experimental point of view at present there is evidence that in solid  $^4\text{He}$ , a vacancy concentration below 0.4% cannot be ruled out [32]. However one should also note that one study [6] has concluded that the vacancy concentration at low temperatures in a system of  $^4\text{He}$  atoms is exceedingly small. On the other hand some theoretical calculations [5, 11] have shown that a perfect  $^4\text{He}$  solid will not exhibit supersolidity and others [7, 29, 33] indicate that some kind of defects should be present. In brief, even though the experimental observation of a NCRI has been confirmed in many laboratories [23, 28, 31] a consensual theoretical interpretation of the results remains to be found.

We determine the vacancy concentration by computing the vacancy-formation free energy  $f$  with the RW method. This is an approach that has shown to be very effective for the computation of defect thermal equilibrium concentrations in classical solids [13, 15, 22]. We will be showing that this method can be applied equally well to quantum solids formed by bosons in the ground state.

Since the exact wave function  $\Psi$  describing the ground state of any system of bosons can always be written as a real nodeless function [1, 9, 26, 27], without loss of generality, it is possible to write

$$\Psi^2(R) = \frac{\exp[-U(R)]}{\mathcal{Q}_N}, \quad (2)$$

where  $\mathcal{Q}_N$  is a normalization factor. The factor  $\exp(-U(R))$  can be formally thought of as a Boltzmann factor at  $k_B T = 1$  with  $k_B$  being the Boltzmann constant and  $T$  the absolute temperature. In the same way, we can identify  $\mathcal{Q}_N$  as the configurational partition function of a fictitious classical system. Accordingly, if the probability density of the classical system predicts a given equilibrium vacancy concentration at  $k_B T = 1$ , this is the expected vacancy

concentration of the quantum system at  $T = 0$  K. In this way, the RW method, which was developed for the calculation of classical free energies of the form  $-\ln \mathcal{Q}_N$ , allows the determination of the equilibrium vacancy concentration of the quantum crystal in its ground state. In case the quantum crystal behaves like a Mott “insulator” [2], the formation free energy in the classical system will be very large, giving a ground-state equilibrium vacancy concentration that is essentially equal to zero. Otherwise, it will be such that the concentration is finite.

In the next section we discuss how the vacancy concentration is computed for the particular quantum solid described by a wave function of the Jastrow form of (1). Furthermore, it delineates the RW method used to determine the formation free energy of a vacancy by taking into account both harmonic and anharmonic effects. Section 3 describes the computational details of the calculations and in Sect. 4 we discuss the obtained results. We conclude with a summary in Sect. 5.

## 2 Methodology

It can be shown that the wave function  $\psi_J(R)$  of the Jastrow form of (1) is the exact ground-state solution of the many-body Schrödinger equation that depends on the first  $u'$  and second derivative  $u''$  of the pseudopotential  $u$

$$\begin{aligned} \mathcal{H} = & \sum_{i=1}^N -\frac{\hbar^2}{2m} \nabla_i^2 + \frac{\hbar^2}{m} \sum_{i<j} \left[ u'(r_{ij}) \left( u'(r_{ij}) - \frac{2}{r_{ij}} \right) - u''(r_{ij}) \right] \\ & + \frac{\hbar^2}{m} \sum_{i<j<k} [u'(r_{ij})u'(r_{ik})\hat{\mathbf{r}}_{ij} \cdot \hat{\mathbf{r}}_{ik} + \mathcal{P}_{ijk}], \end{aligned} \quad (3)$$

where  $\hat{\mathbf{r}}_{ij}$  and  $\hat{\mathbf{r}}_{ik}$  are unit vectors associated with the coordinate differences of the particle pairs  $(i, j)$ , and  $(i, k)$ , respectively and  $\mathcal{P}_{ijk}$  represents the remaining cyclic permutations  $\{ijk\}$  of the three-body term.

It is easy to see that the square of the Jastrow function  $\psi_J^2$  can be rewritten in the form of (2) if we make

$$U(R) = \sum_{i<j} u(r_{ij}). \quad (4)$$

Once we consider the above expression, it is straightforward to realize that  $\psi_J^2(R)$  without the normalization factor  $\mathcal{Q}_N$  is formally equivalent to the Boltzmann factor of a classical many-body system with potential energy function  $U(R)$  at  $k_B T = 1$ . Through the whole paper all quantities that have the dimension of energy are measured in arbitrary energy units. As Hodgdon and Stillinger [16] we use

$$u(r) = \left( \frac{b}{r} \right)^6, \quad (5)$$

where  $b$  is a parameter.

## 2.1 Vacancy Thermodynamics in Classical Systems

The determination of the thermal equilibrium concentration of vacancies in a classical crystal requires the minimization of its free energy with respect to the total number of vacancies  $n$  [4]. Let  $f$  be the formation free energy of a monovacancy in the crystal, defined as the free-energy difference

$$f = F(N - 1) - \frac{N - 1}{N} F(N), \quad (6)$$

where  $F(N - 1)$  and  $F(N)$  are respectively the Helmholtz free energies of a crystal containing  $N - 1$  particles and a single vacancy, and a defect-free crystal of  $N$  particles. It can then be shown [4] that in thermodynamic equilibrium the vacancy concentration  $c$  is then given by

$$c \equiv \frac{n}{N} = \exp\left[-\frac{f}{k_B T}\right]. \quad (7)$$

## 2.2 Free-Energy Calculations

### 2.2.1 Reversible-Work Method

In order to determine the vacancy concentration we need to compute the vacancy-formation free energy  $f$ . Since it is a thermal quantity that cannot be expressed in terms of an ensemble average, it cannot be computed directly using Monte Carlo (MC) or Molecular Dynamics sampling methods. As a result, free energies are usually determined using indirect strategies, in which free-energy *differences* between two systems can be computed by evaluating the work associated with a reversible process that connects these two systems. This approach has shown to be very effective for the computation of defect thermal equilibrium concentrations in classical solids [13, 15, 22].

We compute the free energy  $f$  using the reversible work method. Its main idea is to take a reference system, for which the free energy is known, and perform a connection to the one of interest by means of a varying coupling parameter  $\lambda$ . A typical functional form of this coupling is given by the Hamiltonian

$$H(\lambda) = \lambda H_0 + (1 - \lambda) H_{\text{ref}}, \quad (8)$$

where  $H_0$  and  $H_{\text{ref}}$  represent the Hamiltonians of the system of interest and of reference, respectively. Note that this form allows a continuous switching between  $H_{\text{ref}}$  and  $H_0$  by varying the parameter  $\lambda$  between 0 and 1. The free-energy difference is then given by the *reversible* work  $W_{\text{rev}}$  [15]

$$W_{\text{rev}} \equiv F_0 - F_{\text{ref}} = \int_0^1 d\lambda \left\langle \frac{\partial H}{\partial \lambda} \right\rangle, \quad (9)$$

where the brackets indicate an equilibrium average in a statistical ensemble. This integration gives the total work done by the generalized force  $\partial H / \partial \lambda$ . Since it involves equilibrium averages of the system at all times, it reflects a reversible process.

In principle, the numerical evaluation of the work integral equation (9) can be done by a series of independent equilibrium simulations, each carried out at a different value of the coupling parameter  $\lambda$  between 0 and 1. In practice, however, it has shown beneficial to

estimate the work integral along a single, nonequilibrium simulation during which the value of  $\lambda$  changes dynamically. In this case the reversible work  $W_{\text{rev}}$  is estimated in terms of the *irreversible* work estimator

$$W_{\text{irr}} = \int_0^{t_{\text{sim}}} dt' \left[ \frac{d\lambda}{dt} \right]_{t'} \left[ \frac{\partial H(\{\mathbf{r}_i\}, \lambda)}{\partial \lambda} \right]_{\lambda(t')}, \quad (10)$$

where  $t'$  represents the “time” coordinate that describes the dynamical evolution of the coupling parameter  $\lambda(t)$ , and  $t_{\text{sim}}$  is the total duration of the switching process.

Since the dynamical process above is intrinsically irreversible, the work estimator of (10) is *biased*, subject to a positive systematic error associated with the dissipative entropy production inherent to nonequilibrium processes. As a result, it will represent an upper bound to the value of the reversible work  $W_{\text{rev}}$  and, consequently, the free-energy difference  $F_0 - F_{\text{ref}}$ . Fortunately the systematic error can be readily eliminated, as long as the nonequilibrium process remains within the regime of linear response. In this regime, the systematic error is independent of the switching process direction, *i.e.*, the entropy production is equal for the forward ( $\lambda = 0 \rightarrow 1$ ) and backward ( $\lambda = 1 \rightarrow 0$ ), processes [20, 21]. In this way, we can obtain an unbiased estimate for  $W_{\text{rev}}$  according to

$$W_{\text{rev}} = \frac{1}{2} [W_{\text{irr}}(\lambda = 0 \rightarrow 1) - W_{\text{irr}}(\lambda = 1 \rightarrow 0)], \quad (11)$$

subject only to statistical errors.

The initial step toward computing the formation free energy of a vacancy, (6), utilizing the RW approach involves the calculation of the free energy  $F(N)$  of a defect-free crystal with  $N$  particles. The strategy will be to use the Einstein crystal, of which the free energy  $F_{\text{Einst}}$  is known analytically, as a reference system [15]. In this manner, employing the potential energy expression of (4) and (5), the particular form of the coupled Hamiltonian (8) becomes

$$H(R; \lambda) = \lambda \left[ \sum_{i < j}^N \left( \frac{b}{r_{ij}} \right)^6 \right] + (1 - \lambda) \left[ U(R^{(0)}) + \frac{1}{2} \sum_{i=1}^N \kappa (\mathbf{r}_i - \mathbf{r}_i^{(0)})^2 \right], \quad (12)$$

where  $R^{(0)} \equiv \{\mathbf{r}_i^{(0)} \mid i = 1, \dots, N\}$  represents the equilibrium lattice positions of the  $N$  particles and  $\kappa$  is a spring constant.

Since  $W_{\text{rev}}$  is the difference of the Helmholtz free energy between the systems of interest and of reference, the free energy of the defect-free crystal is given by

$$F(N) = W_{\text{rev}} + F_{\text{Einst}}. \quad (13)$$

It is convenient to fix the center of mass of the system during the switching process. In the presence of this constraint, the free energy of the Einstein crystal is given by [15]

$$F_{\text{Einst}} = U(R^{(0)}) - \frac{3}{2} k_B T N \ln \left[ \frac{2\pi k_B T}{\kappa} \right] - \frac{3}{2} k_B T \ln \left[ \frac{\kappa}{8\pi^2 (k_B T)^2} \right]. \quad (14)$$

The value of the spring constants  $\kappa$  is adjusted such that the mean-square displacement of the harmonic oscillators are approximately equal to those of the particles in the system of interest.

In the second step we estimate the free energy  $F(N - 1)$  of the system containing a single vacancy. In order to apply the RW method we use a similar strategy to the one employed

to compute  $F(N)$ . In this case, the parameter  $\lambda$  controls the strength to which a single particle is tied to an harmonic oscillator and its interaction with all the others. The coupled Hamiltonian for this process is given by

$$H(\{\mathbf{r}\}; \lambda) = \sum_{\substack{i < j \\ (i \neq k)}}^N \left( \frac{b}{r_{ij}} \right)^6 + \lambda \sum_{\substack{i \\ (i \neq k)}}^N \left( \frac{b}{r_{ik}} \right)^6 + (1 - \lambda) \frac{1}{2} \kappa (\mathbf{r}_k - \mathbf{r}_k^{(0)})^2, \quad (15)$$

where the index  $k$  stands for the particle that is turned on and off as  $\lambda$  is varied between 0 and 1. The final term, the single harmonic oscillator, describes the final state of particle  $k$  when it has been totally decoupled from the remainder of the system. It is included in (15) to prevent the decoupled particle  $k$  from drifting freely through the system [22]. As before, the center of mass is held fixed during the switching simulations. Furthermore, it is convenient [16] to maintain the particle density  $\rho$  of the system constant. This is done by varying the size  $L$  of the simulation box as the value of  $\lambda$  is changed. Specifically, we set

$$L(\lambda) = \sqrt[3]{\frac{N - 1 + \lambda}{\rho}}, \quad (16)$$

such that the density of *interacting* particles remains constant as  $\lambda$  is switched on and off.

A final concern involves the applicability of the method when the vacancy diffusion may interfere with the RW process. In this situation, one of the twelve nearest-neighbor particles of the decoupled particle may move into the vacant lattice site by means of a diffusion event, which may lead to singularities in the driving force. An adequate solution to this problem is to constrain the motion of the neighboring particles such that they are forced to remain within their respective Wigner-Seitz primitive cells [22].

From the coupled Hamiltonian in (15) we determine the driving force  $\partial H / \partial \lambda$  and compute the reversible work  $W'_{\text{rev}}$  required to turn off the interactions between particle  $k$  and the remainder of the system and turn it into an independent harmonic oscillator. As in the previous case, the switching process is carried out in both directions to eliminate the systematic error. Accordingly,  $F(N - 1)$  is obtained through

$$F(N - 1) = W'_{\text{rev}} + F(N) - F_{\text{osc}}, \quad (17)$$

where  $F_{\text{osc}}$  is the free energy of a single harmonic oscillator, given by

$$F_{\text{osc}} = -\frac{3}{2} k_B T \ln \left[ \frac{2\pi k_B T}{\kappa} \right]. \quad (18)$$

Finally, combining the results of (13), and (17) we compute the vacancy formation free energy through (6). The corresponding zero-point vacancy concentration is then calculated by (7).

## 2.2.2 Harmonic Approximation

The harmonic approximation [25] is a method that allows one to estimate the vacancy-formation free energy without sampling configurations from a statistical ensemble. The central idea of this approximation is to write the free energy as the sum of static potential energy plus a finite-temperature part involving the vibrational normal mode frequencies  $\omega_i$ , where  $i = 1, \dots, 3N - 3$ .

In this manner [16], the vacancy formation  $f$  is given by

$$f = U(N-1) - \left(\frac{N-1}{N}\right)U(R^{(0)}) + k_B T \sum_{i=1}^{3N-6} \ln \left[ \frac{\omega_i(N-1)}{k_B T} \right] - \left(\frac{N-2}{N-1}\right)k_B T \sum_{i=1}^{3N-3} \ln \left[ \frac{\omega_i(N)}{k_B T} \right], \quad (19)$$

where  $U(N-1)$  represent the static potential energies of the crystal containing a single vacancy. The last two terms represent the vibrational parts of the crystals with and without vacancy, respectively. In practice the vibrational frequencies are obtained by diagonalizing the Hessian matrix of the potential-energy functions. We want to compare results of such harmonic calculation [16] with those obtained by the RW method that do not neglect anharmonic effects.

### 3 Computational Details

All calculations were carried out using cubic simulation cells with a fcc structure and containing numbers of particles  $N$  varying between 108 and 1372. To eliminate surface effects, we apply standard periodic boundary conditions and invoke the minimum-image convention [15]. In order to be consistent with a continuous and differentiable wave function we force the pseudopotential to be equal to zero for interatomic distances equal to half the side of the simulation cell,  $r = L/2$ . A convenient way to do is to slightly modifying the pseudopotential  $u(r)$  of (5) according to [35]

$$u(r) \rightarrow \tilde{u}(r) = u(r) + u(L-r) - 2u(L/2). \quad (20)$$

The criterion for our choice of the density is to have a stable fcc phase for the system of soft spheres at  $k_B T = 1$ . Based on the results for the soft sphere phase diagram by Prestipino et al. [30] we have performed most of our calculations at a density  $\rho = 2.44b^{-3}$ , which is slightly above the melting value for this system. Few additional calculations at lower densities have been done as well. However as our results will show, the precise value of the density does not affect our conclusions.

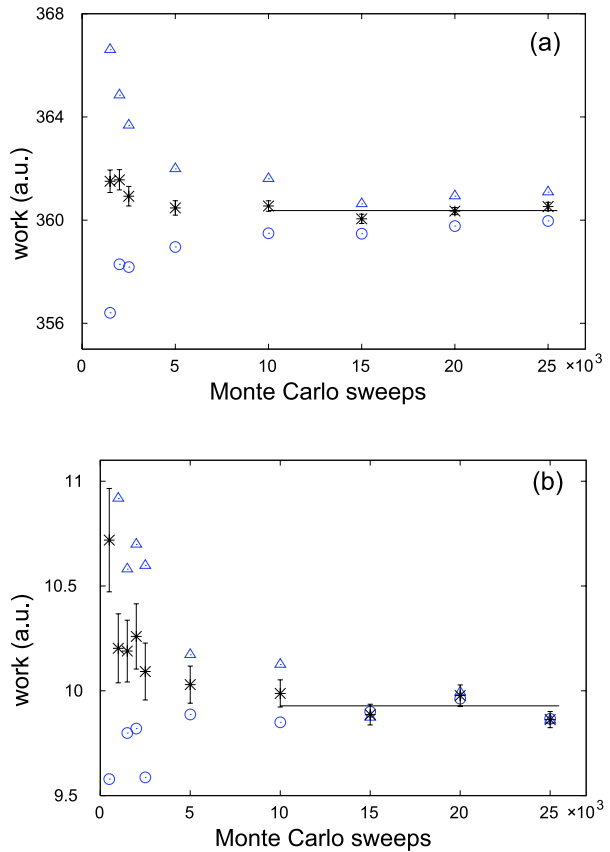
We apply the Metropolis algorithm to sample configurations from  $\psi_2^2(R)$ . In RW simulations the switching parameter is varied linearly according to  $\lambda = t/t_{\text{sim}}$  (forward process) or  $\lambda = 1 - t/t_{\text{sim}}$  (backward process). It is important to remember that one must always start the RW process from an equilibrated system. Accordingly, every run for both switching directions was preceded by an equilibration of at least  $5 \times 10^3 MC$  sweeps before computing the work of (10). As mentioned earlier, in order to guarantee that the RW results obtained from nonequilibrium processes are bias-free, we have computed the irreversible work estimators for both switching directions as a function of the total duration  $t_{\text{sim}}$  of the simulations. At each run we determine averages of the irreversible work estimator over 30 switching processes.

### 4 Results and Discussion

The graphs displayed in Fig. 1 show the average values of the forward and backward irreversible work estimators and the unbiased estimator of (11) as a function of the total process

**Fig. 1** (Color online)

Irreversible work calculations associated with the process of transforming the interacting, defect-free solid into an Einstein crystal **(a)** and the process of introducing a monovacancy in the solid **(b)** as a function of the process duration  $t_{\text{sim}}$  measured in MC sweeps. Results are displayed for the forward processes ( $\Delta$ ), backward processes ( $\circ$ ), and the corresponding unbiased estimator of (11) (\*). Each point was obtained as the average over thirty independent simulations carried out with  $N = 500$  particles. The *solid line* is an average of the last four values of the unbiased work estimator for which the processes have reached the linear-response regime



duration  $t_{\text{sim}}$ . These results monitor the convergence of the RW calculations for the defect-free crystal (panel a) and for the reversible vacancy insertion process (panel b) obtained for a cell of 500 particles at  $k_B T = 1$ . From the results we see that  $t_{\text{sim}} \approx 10^4$  sweeps is sufficiently long for the linear response regime to be reached in both cases, for which the unbiased estimator reaches convergence. The horizontal lines on the graphs are averages of the last four values of the reversible work in that region. Based on these results, all subsequent RW switching simulations based on different numbers of particles and temperatures were carried out with  $t_{\text{sim}} = 1.5 \times 10^4$  MC sweeps.

The results depicted in Fig. 2 show a comparison between the vacancy-formation free energy as a function of temperature as obtained using the RW and HA methods for a cell of 500 particles. The plot clearly demonstrate the significance of anharmonicity. As expected, for low temperatures, anharmonic effects are small and both the HA and the RW method converge to the same formation free-energy value for temperatures tending to zero. As temperature increases, however, anharmonicity becomes increasingly important and the deviation between the RW and HA results becomes significant. Specifically, at  $k_B T = 1$ , when the classical and quantum description of the system are formally equivalent, anharmonic effects are responsible for a reduction of about 25% in the value of the vacancy-formation free energy compared to the HA result. The anharmonic effects are associated with the significant zero-point motion in the quantum system at  $T = 0$  K. The importance of this motion can be



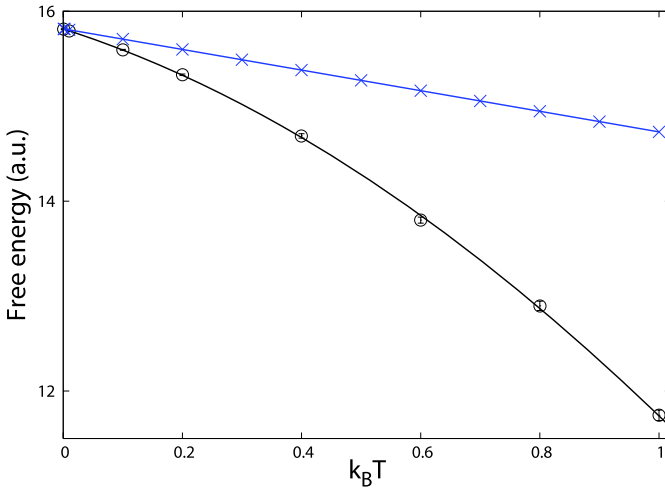


**Fig. 2** (Color online) Vacancy-formation free energy as a function of temperature. Results were obtained for  $\rho = 2.44b^{-3}$  and  $N = 500$ . HA ( $\times$ ) and RW ( $\circ$ ) results. The *lines* are guides to the eyes

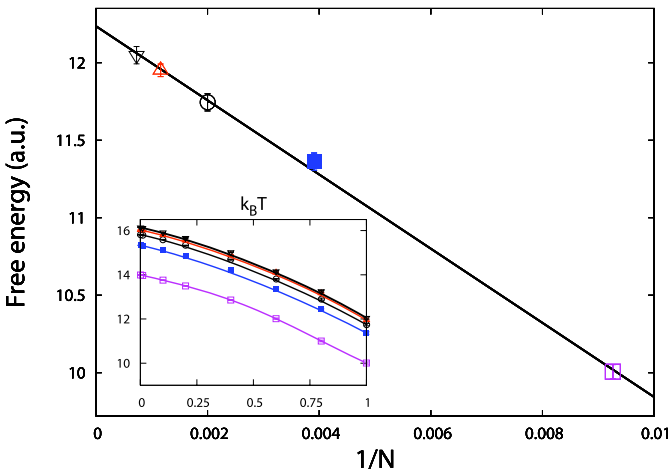


**Fig. 3** (Color online) Vacancy-formation free energy as a function of system size at  $k_B T = 1$ . The *straight line* was obtained through a least-square linear fit. Results obtained for  $\rho = 2.44b^{-3}$  and  $N = 108$  ( $\square$ ),  $N = 256$  ( $\blacksquare$ ),  $N = 500$  ( $\circ$ ),  $N = 864$  ( $\triangle$ ) and  $N = 1372$  ( $\nabla$ ). *Inset* shows the formation free energy as a function of  $k_B T$  for the mentioned system sizes

approximately estimate in terms of the formation entropy of the classical system,  $s = -\frac{\partial f}{\partial T}$ , at  $k_B T = 1$ , which can be computed from the slope of the formation free-energy curves. The resulting values give  $s = 1.1k_B$  and  $s = 6.0k_B$  for the HA and RW results, respectively. This difference of almost a factor of six is another clear indication of the importance of anharmonicity in the system.

To assess the influence of finite-size effects, we computed the RW vacancy-formation free energy at  $k_B T = 1$  for different cell sizes, ranging from  $N = 108$  to  $N = 1372$  particles. The results are shown in Fig. 3 that plots the formation free energy as a function of  $1/N$ .

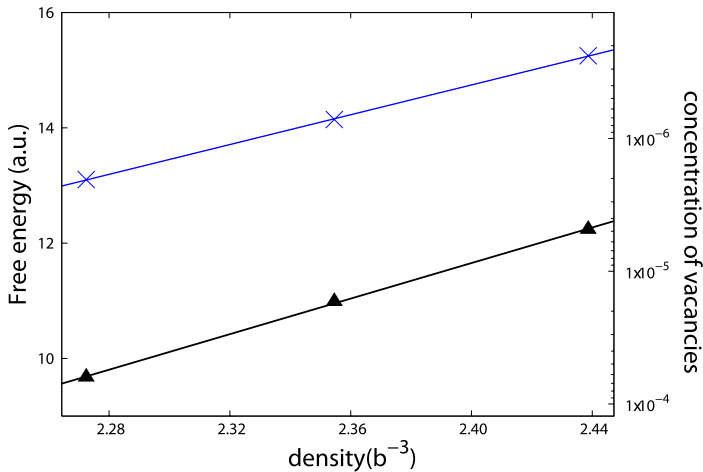


**Fig. 4** (Color online) Extrapolated vacancy-formation free energy as a function of  $\rho$  at  $k_B T = 1.0$ , the scale at the right side gives the corresponding vacancy concentration. Results obtained using the RW method (▲) and the HA (×). Lines are plotted to guide the eyes. The error bars are smaller than the size of used symbols

The inset shows the full formation free-energy versus temperature curves for different cell sizes. The extrapolated vacancy-formation free energy when  $1/N \rightarrow 0$  is  $f = 12.24$  a.u. at the density  $\rho = 2.44b^{-3}$ .

The determination of the extrapolated vacancy-formation free energy  $f$  at  $k_B T = 1$  now allows us to compute the zero-point vacancy concentration, (7), for the system described by the wave functions of (1) and (5). The results are shown in Fig. 4, which plots the extrapolated vacancy-formation free energy as well as the associated vacancy concentration as a function of the density, using both the RW and HA methods. The effects of anharmonicity are clearly visible, reducing the formation free energy by  $\sim 20$ – $25\%$  and increasing the vacancy concentration by more than an order of magnitude. At the density  $\rho = 2.27b^{-3}$ , where the system is still a solid, the value of the free energy  $f = 9.67$  a.u. corresponds to a vacancy concentration of  $6.3 \times 10^{-5}$ .

## 5 Conclusions

In this paper we have shown that the reversible-work method can be successfully applied to the calculation of the zero-point vacancy concentration of a simple quantum solid model. Moreover and more importantly, we demonstrate that anharmonic effects play a significant role in the determination of this quantity. Specifically, we find that anharmonicity leads to a decrease of the formation free energy of about  $25\%$ , resulting in a vacancy concentration that is more than an order of magnitude larger compared to the harmonic results.

The RW approach we have used in this work is not limited to the investigation of vacancies alone. It can also be used to investigate the concentration of other species of defects such as interstitials and defect complexes formed by multiple vacancies and interstitials. It is important to emphasize that the RW methodology is not restricted to the simple wave function of the Jastrow form utilized here, but that it can be applied to any other functional forms such as the shadow wave function [34], which has been shown to give one of the best variational descriptions of solid  $^4\text{He}$ .

In summary, even if the analysis of the model system we have presented does not intend to provide results for a real quantum solid like  $^4\text{He}$  it has demonstrated quantitatively how anharmonic effects are important and that certainly they have to be taken into account if one wants to investigate the vacancy concentration in this quantum crystal. Moreover this paper also shows that the calculation of defect concentrations in quantum solids formed by bosons can be treated by the RW method in a reliable and efficient way.

**Acknowledgements** The authors gratefully acknowledge financial support from the Brazilian agencies FAPESP, CNPq and CAPES. Part of the computations were performed at the CENAPAD high-performance computing facility at Universidade Estadual de Campinas.

## References

1. Anderson, P.W.: Physics of a superfluid solid. [arXiv:cond-mat/0504731v1](https://arxiv.org/abs/cond-mat/0504731v1) (2005)
2. Anderson, P.W., Brinkman, W.F., Huse, D.A.: Thermodynamics of an incommensurate quantum crystal. *Science* **310**, 1164 (2005)
3. Andreev, A.F., Lifshitz, I.M.: Quantum theory of defects in crystals. *Sov. Phys. JETP* **29**, 1107 (1969)
4. Ashcroft, N.W., Mermin, N.D.: *Solid State Physics*. Brooks/Cole (1976)
5. Boninsegni, M., Prokof'ev, N.V., Svistunov, B.V.: Superglass phase of  $^4\text{He}$ . *Phys. Rev. Lett.* **96**, 105301 (2006)
6. Boninsegni, M., Kuklov, A.B., Pollet, L., Prokof'ev, N.V., Svistunov, B.V., Troyer, M.: Fate of vacancy-induced supersolidity in  $^4\text{He}$ . *Phys. Rev. Lett.* **97**, 080401 (2006)
7. Boninsegni, M., Kuklov, A.B., Pollet, L., Prokof'ev, N.V., Svistunov, B.V., Troyer, M.: Luttinger liquid in the core of a screw dislocation in helium-4. *Phys. Rev. Lett.* **99**, 035301 (2007)
8. Burns, C.A., Goodkind, J.M.: Search for evidence of the influence of vacancies on the thermal conductivity of solid  $^4\text{He}$ . *J. Low Temp. Phys.* **93**, 15 (1993)
9. Campbell, C.E.: The structure of quantum fluids. In: Croxton, C.A. (ed.) *Progress in Liquid Physics*. Wiley, New York (1977)
10. Chester, G.V.: Speculations on Bose-Einstein condensation and quantum crystals. *Phys. Rev. A* **2**, 256 (1970)
11. Clark, B., Ceperley, D.M.: Off-diagonal long-range order in solid  $^4\text{He}$ . *Phys. Rev. Lett.* **96**, 105302 (2006)
12. Day, J., Beamish, J.: Low-temperature shear modulus changes in solid  $^4\text{He}$  and connection to supersolidity. *Nature* **450**, 853 (2007)
13. de Debiaggi, S.R., de Koning, M., Monti, A.M.: Theoretical study of the thermodynamic and kinetic properties of self-interstitials in aluminum and nickel. *Phys. Rev. B* **73**, 104103 (2006)
14. Foiles, S.M.: Evaluation of harmonic methods for calculating the free energy of defects in solids. *Phys. Rev. B* **49**, 14930 (1994)
15. Frenkel, D., Smit, B.: *Understanding Molecular Simulations: From Algorithms to Applications*. Academic Press, San Diego (2002)
16. Hodgdon, J.A., Stillinger, F.H.: Equilibrium concentration of point defects in crystalline  $^4\text{He}$  at 0 K. *J. Stat. Phys.* **78**, 117 (1995)
17. Kim, E., Chan, M.H.W.: Observation of superflow in solid helium. *Science* **305**, 1941 (2004)
18. Kim, E., Chan, M.H.W.: Probable observation of a supersolid helium phase. *Nature* **427**, 225 (2004)
19. Kim, E., Chan, M.H.W.: Supersolid helium at high pressure. *Phys. Rev. Lett.* **97**, 115302 (2006)
20. de Koning, M.: Optimizing the driving function for nonequilibrium free-energy calculations in the linear regime: a variational approach. *J. Chem. Phys.* **122**, 104106 (2005)
21. de Koning, M., Cai, W., Antonelli, A., Yip, S.: Efficient free energy calculations by simulation of non-equilibrium processes. *Comput. Sci. Eng.* **2**, 88 (2000)
22. de Koning, M., de Debiaggi, S.R., Monti, A.M.: Atomistic calculation of vacancy-formation free energies by reversible vacancy creation. *Phys. Rev. B* **70**, 054105 (2004)
23. Kondo, M., Takada, S., Shibayama, Y., Shirahama, K.: Observation of non-classical rotational inertia in bulk solid  $^4\text{He}$ . *J. Low Temp. Phys.* **148**, 695–699 (2008)
24. MacFarland, T., Vitiello, S.A., Reatto, L., Chester, G.V., Kalos, M.H.: Trial shadow wave function for the ground state of  $^4\text{He}$ . *Phys. Rev. B* **50**, 13577 (1994)
25. Maradudin, A.A., Montroll, E.W., Weiss, G.H., Ipatova, I.P.: *Theory of Lattice Dynamics in the Harmonic Approximation*, 2nd edn. Academic, New York (1971)

26. McMillan, W.L.: Ground state of liquid  $^4\text{He}$ . *Phys. Rev.* **138**, A442–A451 (1965)
27. Penrose, O., Onsager, L.: Bose-Einstein condensation and liquid helium. *Phys. Rev.* **104**, 576–584 (1956)
28. Penzev, A., Yasuta, Y., Kubota, M.: Annealing effect for supersolid fraction in  $^4\text{He}$ . *J. Low Temp. Phys.* **148**, 677–681 (2007)
29. Pollet, L., Boninsegni, M., Kuklov, A.B., Prokof'ev, N.V., Svistunov, B.V., Troyer, M.: Superfluidity of grain boundaries in solid  $^4\text{He}$ . *Phys. Rev. Lett.* **98**, 135301 (2007)
30. Prestipino, S., Saija, F., Giaquinta, P.V.: Phase diagram of softly repulsive systems: the Gaussian and inverse-power-law potentials. *J. Chem. Phys.* **123**, 144110 (2005)
31. Rittner, A.S.C., Reppy, J.D.: Disorder and the supersolid state of solid  $^4\text{He}$ . *Phys. Rev. Lett.* **98**, 175302 (2007)
32. Simmons, R., Blasdel, R.: Precise neutron diffraction study of hcp and bcc  $^4\text{He}$ . In: Meeting of the American Physical Society (2007). URL <http://meetings.aps.org/link/BAPS.2007.MAR.P31.12>
33. Toner, J.: Quenched dislocation enhanced supersolid ordering. *Phys. Rev. Lett.* **100**, 035302 (2008)
34. Vitiello, S., Runge, K., Kalos, M.H.: Variational calculations for solid and liquid  $^4\text{He}$ . *Phys. Rev. Lett.* **60**, 1970–1973 (1988)
35. Vitiello, S.A., Schmidt, K.E.: Variational methods for  $^4\text{He}$  using a modern He-He potential. *Phys. Rev. B* **60**, 12342 (1999)